

Passive dynamic walking model with upper body

M. Wisse*, A. L. Schwab and F. C. T. van der Helm

*Biped Laboratory, Faculty of Mechanical Engineering, Delft University of Technology, Mekelweg 2,
NL-2628 CD Delft (The Netherlands)*

(Received in Final Form: April 14, 2004)

SUMMARY

This paper presents the simplest walking model with an upper body. The model is a passive dynamic walker, i.e. it walks down a slope without motor input or control. The upper body is confined to the midway angle of the two legs. With this kinematic constraint, the model has only two degrees of freedom. The model achieves surprisingly successful walking results: it can handle disturbances of 8% of the initial conditions and it has a specific resistance of only 0.0725(–).

KEYWORDS: Passive dynamic walking; Biped; Passive upper body.

I. INTRODUCTION

How much of the human walking motion can be modeled with passive dynamics? The more we can, the more likely we are to find simple designs for e.g. walking rehabilitation or entertainment robots. This question arose when Mochon and McMahon¹ discovered that the free swing motion of the human leg can be modeled quite convincingly (though not completely²) as a passive double pendulum.

In the late eighties, McGeer³ showed that passive dynamic modeling is not only suitable for the swing leg motion, but for the stance leg motion as well. He built models and prototypes which he called ‘passive dynamic walkers’, that can walk down a shallow slope with no actuation and no control. Increasingly complex prototypes⁴ show that passive dynamic walking results in a particularly elegant and natural bipedal gait.

Passive dynamic walking provides two interesting features: inherent stability and low energy consumption. First, for certain parameter values, the passive models can resist small disturbances without the need for control. If human locomotion is based on passive walking, this could explain why keeping our balance seems so easy for us. Second, the energy consumption of passive walkers (gravitational energy from walking downhill) is much lower than that of conventional bipedal robots; it is actually even lower than that of human walking. All in all, passive dynamic walking is an attractive concept for models of human walking.

However, there is one major shortcoming. Up till now, none of the existing passive dynamic walking models had a fully passive upper body. These models either consist only of a pair of legs, or they have an upper body with active stabilization.^{5,6} In contrast, for applicable results for instance in the fields of entertainment or rehabilitation, the upper body is an essential part of the system. Recognizing this, many researchers work on advanced control paradigms for the hip joint.^{7–9} It would be advantageous, however, if the upper body could be stabilized in a completely passive manner. Before we endeavor to build a prototype with such an upper body, we will demonstrate theoretically the feasibility with a computer model.

The research aim is to incorporate the upper body in the concept of Passive Dynamic Walking. The goal of this paper is to present a fully passive walking model with an upper body, and to investigate the effects of the parameters of the upper body on the walking characteristics, such as stability and energy efficiency.

II. PASSIVE WALKING MODEL WITH UPPER BODY

The goal of this research is a passive walking model with an upper body. This model should be as simple as possible for the sake of a minimal set of parameters, so a natural starting point would be the ‘simplest walking model’ of Garcia *et al.*¹⁰ The simplest walking model consists of two rigid massless legs, with small pointmasses m_f as feet and a finite pointmass at the frictionless hip joint. For slopes up to 0.015 (rad), this model performs a stable walk downhill.

Their model deserves an accordingly simple upper body. A pointmass will do, connected to a rigid, massless stick that rotates around the hip joint (Fig. 1). The upper body is parameterized with a body length l_b and body mass m_b . The default parameter values are somewhat arbitrarily chosen to have some relevance to human walking or to future prototypes (Table I). We made the parameter values dimensionless for comparison with other models: all sizes are scaled with the leg length, so that the leg length is 1(–), and all masses are scaled with the sum of the pelvis mass and the upper body mass, so that the pelvis mass is $1 - m_b(-)$. The foot mass is not included in this sum for reasons of compatibility with older models.¹¹ Time is scaled so that the resulting gravity is 1(–). Notice that, because of this scaling, parameters become unit-less, hence the ‘(–)’. There are also two non-human parameters: 1) slope angle γ , with which

* Corresponding author: M. Wisse. E-mail: M.Wisse@wbmt.tudelft.nl.

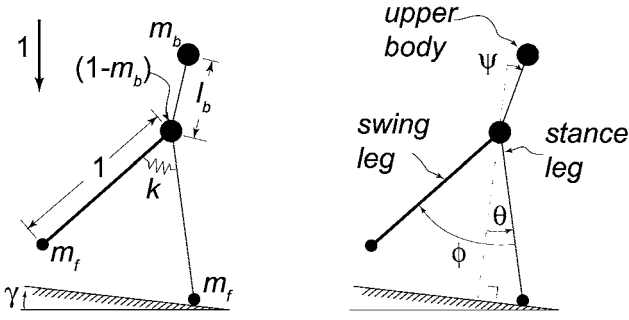


Fig. 1. Model of the simplest walker with upper body; parameters (left) and degrees of freedom (right).

Table I. Default parameter values for the simplest walker with upper body, from a rough estimation of human proportions. The parameters are nondimensionalized by scaling: mass is divided by (pelvis mass + upper body mass), length is divided by leg length, time is divided by $\sqrt{\text{leg length}/\text{gravity}}$.

parameter	symbol	human approx.	scaled
Foot mass	m_f	7 (kg)	0.1 (—)
Upper body mass	m_b	49 (kg)	0.7 (—)
(Pelvis mass)	$(1 - m_b)$	21 (kg)	0.3 (—)
Leg length	—	1 (m)	1 (—)
Body length	l_b	0.4 (m)	0.4 (—)
Hip spring stiffness	k	—	0.4 (—)
Slope angle	γ	—	0.0725 (rad)

we can tune the walking speed, and 2) hip spring stiffness k , which allows tuning of the step frequency. The spring will turn out to be necessary for stable walking, as will be described in Section IV(C). With the default parameter values according to Table I, the model walks with human-like speed and step length (see Section IVA).

As such, the model would have three degrees of freedom (Fig. 1): absolute stance leg angle θ (counter-clockwise), relative swing leg angle ϕ (clockwise), and absolute body angle ψ (clockwise). However, the upper body is then just an inverted pendulum jointed around the hip. Without any active control acting on it, one can expect that it will not be kept upright passively. To keep a fully passive upper body upright, A. Ruina (personal communication) suggests four possibilities:

- (i) Use a light upper body that has its actual center of mass *below* the hip. This option is not very useful in realistic prototypes.
- (ii) Use springs that keep the upper body upright.⁶ This also has the advantage that it should produce more efficient walking by making the steps smaller at a given speed.¹²
- (iii) Use a compass mechanism: a kinematic coupling that keeps the body midway between the two legs (Fig. 2).
- (iv) Keep the model as it is, and hope that for some special mass distribution suddenly a stable gait emerges.

Intuitively, option three is the most promising because the number of degrees of freedom is reduced, which improves the chances of finding stable walking cycles. Human beings

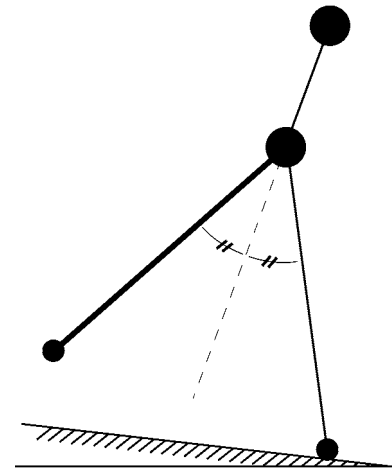


Fig. 2. Kinematic coupling of the upper body to the midway leg angle according to Eq. (1).

Table II. Initial conditions that result in a cyclic walking pattern for the simplest walker with upper body, using the default parameter values (Table I).

θ_0	0.3821 (rad)
$(\phi_0 = 2\theta_0)$	(0.7642 (rad))
$\dot{\theta}_0$	−0.3535 (rad/—)
$\dot{\phi}_0$	0.0736 (rad/—)

do not have such a kinematic coupling, but the assembly of pelvic muscles and reflexes could possibly perform a similar function. Also, such a construction can be found in certain reciprocating gait orthoses.¹³ In robot prototypes such a kinematic coupling can be easily realized. In the model (Fig. 1) it is introduced according to:

$$\psi = \phi/2 - \theta. \quad (1)$$

The other options could provide valuable results, although the first is not interesting as a model for human walking. We intend to investigate options two and four in the future, but in this paper we will focus on the behavior of the model with the compass-like kinematic constraint.

III. RESULTS

A. Walking motion

The walking motion is analyzed with the help of the methods as described in the Appendix. With the default parameter values, the model takes something like a human walking step if started with the initial conditions from Table II. However, due to its quintessential nature our model shares some typical non-human characteristics with Garcia's simplest walking model. First, the feet are no more than points, hence the application point of the ground contact force is at a fixed location during one step. Second, there are no actuators, so that the model will only walk if placed on a slope. Third,

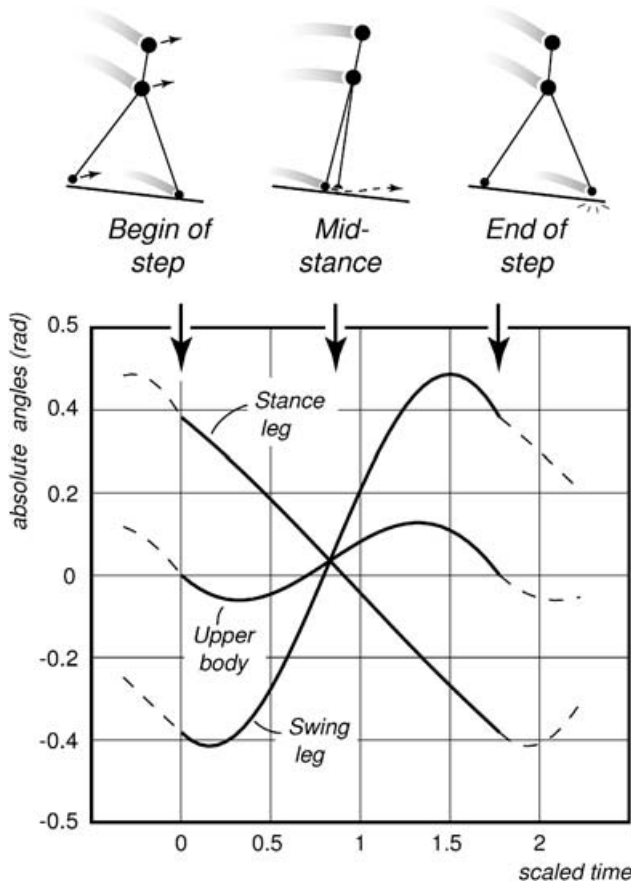


Fig. 3. Cyclic walking motion of the model with upper body. Top: stick figure representation, bottom: absolute angles of stance leg, swing leg, and upper body. The simulation is performed using the default parameter values (Table I).

the legs cannot change length, hence there are not enough degrees of freedom to allow for a double support phase.

The step starts and ends immediately after a ‘heel strike’ (Fig. 3). The hip moves forward like an inverted pendulum with an almost constant speed, while at the same time the swing leg swings to a forward position. Naturally, the kinematic constraint keeps the upper body at the intermediate leg angle. The motion of the swing leg appears to be that of a free pendulum, while actually it is mainly the result of the dynamics of the upper body and the hip spring.

The trajectories of the various pointmasses are no surprise; the hip moves forward on a circular path (often referred to as ‘compass gait’),¹⁴ while the swing foot remains close to the floor. The upper body follows a path almost identical to the hip trajectory at a distance l_b above the hip, only slightly smoother at the heel strike discontinuities. There are two peculiarities. First, the hip trajectory equals that of an inverted pendulum, but its speed does not. Due to the influence of the upper body and the hip spring, the speed of the hip is nearly constant, as can be deduced from the nearly constant stance leg velocity in Fig. 3. Second, the swing foot travels briefly below floor level. Inevitable for a 2D walker with straight legs, we allow this to happen in our simulation. Human beings and our more sophisticated models¹⁵ and prototypes¹⁶ have knees to solve this problem.

With a step length of 0.746(–) and a step time of 1.77(–) the model attains a (scaled) walking velocity of 0.42(–). Back on a human scale this corresponds to 1.3 (m/s). The scaled velocity is the same as the familiar Froude number, $\sqrt{v^2/gl}$, where {Froude number = 1} represents the maximum walking speed for any biped. At higher speeds the foot contact force would become negative, so the biped should switch to running. With a Froude number of 0.42(–) our model is well below that boundary, firmly stepping its way.

The energy consumption of the model at this speed is low. This is usually represented in the non-dimensional form of ‘specific resistance’: energy consumption per distance traveled per kilogram mass per gravity. For passive dynamic walkers the specific resistance is equal to the slope angle γ as gravity is the only means of energy input. So, our model has a specific resistance of 0.0725(–) at a (scaled) speed of 0.42(–). This is much more efficient than human beings walking at the same speed with a specific resistance of approximately 0.38(–),¹⁷ although the comparison is somewhat unfair as muscle efficiency is unaccounted for. Also, this is much more efficient than the current generation of walking robots.

B. Inherent stability

To classify the stability of the walking motion there are two useful but essentially different definitions. First, we can regard stability in its most strict way. The basis is a walking motion in cyclic equilibrium, called a ‘limit cycle’; a certain combination of initial conditions (Table II) keeps repeating itself for all subsequent steps. If started slightly away from the limit cycle, the walking motion is stable if the subsequent step is closer to the limit cycle. Note that this ‘local stability’ requires the existence of a limit cycle, and that only small disturbances are investigated. By application of the method as described in Section F of the appendix we found that the model with the parameter values from Table I and started with the initial conditions from Table II is, indeed, stable for small disturbances.

Second, we can regard the stability of walking in the broadest and most intuitive form: ‘The robot is stable if it does not fall’. We can even allow ourselves to use the formally incorrect term ‘more stable’ for a robot that can handle larger disturbances. Note that this ‘global stability’ does not require the existence of a limit cycle (every step may be different, as long as the robot doesn’t fall), but that it can only be investigated with the costly method of trying out all possible disturbances.

By application of the cell mapping method as described in Section G of the Appendix, we found that the model performs surprisingly well. The model converges to its limit cycle if started with errors as large as 8% on all initial conditions of Table II, compared to 2% for the simplest walking model.¹¹ For certain combinations of errors, the errors can even be much larger. This is inspected by the evaluation of the *basin of attraction* (Fig. 4), the complete set of initial conditions that eventually lead to cyclic walking. For example, the figure shows that cyclic walking with cyclic initial conditions as in Table II, emerges even if the initial step is twice as large, e.g. $\{\theta_0 = 0.75, \dot{\theta}_0 = -0.75, \phi_0 = -1\}$.

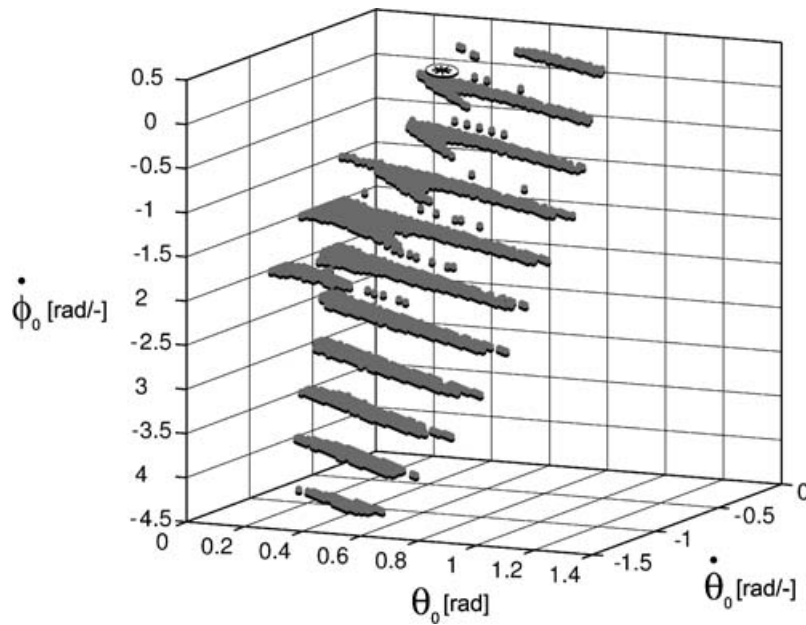


Fig. 4. Basin of attraction of the simplest walking model with upper body. The gray layers of points represent horizontal slices of a 3D region of initial conditions that eventually lead to the cyclic walking motion. The cyclic motion ($\{\theta_0 = 0.3821, \dot{\theta}_0 = -0.3535, \dot{\phi}_0 = 0.0736\}$, Table II) is indicated with a flat asterisk, just above one of the sample slices.

IV. PARAMETER STUDY

A. Slope and spring stiffness; speed and step length

As mentioned in Section II, the model has two parameters that are essential to the model's gait: the slope angle and the hip spring stiffness. Together, they determine the step frequency and the step length, thereby also determining the walking velocity.

First, for a fixed set of mass and length parameters, the step frequency is almost completely determined by the hip spring stiffness. It appears that the swing leg amplitude, step length, slope angle or walking speed all have a negligible influence on the step frequency.^{3,10}

Then, the step length is directly determined by the slope angle; the steeper the slope, the larger the steps. This is a result of the balance between the gravitational energy input and the impulsive energy losses at heel strike. Although a larger step means more energy input, it leads to even more energy loss at heel strike. As a result, the system will automatically converge to a periodic walking motion with a step length that corresponds to the slope angle.

With the hip spring stiffness and the slope angle together, we were able to set both the speed and the step length to human values. It should be noted that these effects are not unique to our model. In fact, Kuo¹² studied these same effects extensively for the simplest walking model to investigate energy aspects of human walking.

B. Upper body height and weight

The upper body is parameterized with body length l_b and body mass m_b . The body mass and the pointmass at the pelvis together always amount to 1 for the purpose of scaling, while the body length is scaled to the length of the leg. The default parameters of Table I are chosen so that the model has some relevance to future prototypes. This section investigates the

model behavior when the upper body is reduced to nothing or significantly enlarged.

The reduction of the upper body size or mass to zero leads to a model like the simplest walker, except that the simplest walker has no hip spring and an infinitesimally small foot mass. For a very small foot mass, no hip spring is necessary, but for a realistic foot mass as in Table I, stable walking cycles only exist if a spring is applied. As stated earlier, the hip spring and slope angle together determine the walking speed and the step length. If we set them so that speed and step length match the original model (Table I), we find that the 'zero-body-model' needs a slope angle of $\gamma = 0.147$ (rad). In other words, the model with upper body is twice as efficient as the same model without upper body! Apart from that, there is not much difference between the gaits of the two models.

Similarly, an increase in the mass or the size of the upper body will provide an even higher walking efficiency. We found that an increase in m_b has a similar effect as an increase in l_b . As an example, we crudely modeled a person carrying a heavy load on the top of the head by setting $m_b = 0.9(-)$ and $l_b = 1(-)$. The hip spring stiffness and slope angle were again adjusted to obtain a human walking speed and step length. The required slope angle is now only $\gamma = 0.0249$ (rad); this model walks about three times more efficiently than with the default parameter values! In general it is clear that the presence of an upper body has a positive influence on the walking efficiency.

The changes of the mass or size of the upper body have little effect on the stability. We investigated the three previously mentioned situations: a) zero upper body mass, b) default parameters (Table I), and c) someone carrying a heavy load on the head ($l_b = 1, m_b = 0.9$). In terms of linearized stability, all three situations are stable for small disturbances. In terms of global stability, the allowable errors on all initial conditions are about 8% for all three situations. It seems

odd that the size or mass of the upper body has no apparent influence on the allowable errors (all 8%), while there is such a large difference with the simplest walking model (only 2%). We believe that this is a result of the increased speed and step frequency; the simplest walking model walks slower than our model, which we tuned to walk with human speed. We intend to investigate this effect in the near future.

C. Limits to stability

Our upper-body walker has a remarkably stable gait if provided with the parameter values from Table I. For certain other parameter values, however, the model has unstable gaits or even no cyclic walking motions at all. Usually this can be solved by sufficiently increasing the hip spring stiffness k , with a few exceptions. At slopes steeper than $\gamma \approx 0.35$ (rad) the equilibrium speed is so high that the stance foot would lose ground contact and the model should start running. The foot mass m_f and the body size and mass l_b and m_b can be chosen arbitrarily small or large; with a high enough value for k the model still walks fine, although this could result in correspondingly small or large step lengths, which in turn could lead to the loss of floor contact.

Inside these boundaries, for each combination of parameter values there exists a minimal value for k that ensures stability. For the model with the default parameter values of Table I, we studied the effect of variations in k on the cyclic walking motion. For $k > 0.218$ we found steady, stable cyclic walking as described in Section III(A). However, for the same value of k there also exists a second, unstable gait. The steps are shorter and faster, and the motion looks like the model is stumbling forward. McGeer and Garcia discovered this second solution for their models and refer to it as the 'short-period gait', as opposed to the normal, stable solution which is termed 'long-period gait'. We are only interested in the last type of gait, the behavior of which we have studied as a function of the parameter value for k .

Above the boundary value, an increase in k results in faster and smaller steps as discussed in section IV(A). If we decrease k below 0.218, we cross a bifurcation to asymmetric gaits, first encountering two-period solutions and for lower k even higher-period solutions. These solutions are still stable. Below $k = 0.162$, we found only unstable gaits or even no cyclic solutions at all. Garcia found a similar bifurcation to chaos for the simplest walking model when increasing the slope above $\gamma = 0.015$ (rad).

We tracked the first bifurcation point over a range of parameter values because that point represents the minimally required value for k to obtain normal, stable walking. The relation between the minimal value for k and the other parameters is not linear, and there is not an obvious and simple non-linear relationship. Qualitatively, the required hip spring stiffness k needs to be increased if l_b , m_b , m_f or γ are increased.

V. CONCLUSION

This paper presented the simplest walking model with a passive upper body. The solution for a fully passive upper body is to confine the upper body angle to the intermediate leg angle with a kinematic coupling. With this kinematic

constraint, the model has only two degrees of freedom, similar to the Simplest Walking Model.

The presence of such an upper body results in a better energy efficiency and in a slightly better robustness against disturbances. A spring in the hip joint is essential for stability. An increase in the hip spring stiffness results in a higher step frequency, whereas the slope angle of the floor determines the step length.

These results are convincing enough to commence the construction of a prototype walking robot with a similar upper body construction.

Acknowledgements

This research is funded by the Dutch national technology foundation STW. Thanks to Richard van der Linde, Jan van Frankenhuyzen, Steve Collins and Dick Plettenburg for many helpful comments.

References

1. S. Mochon and T. A. McMahon, "Ballistic walking", *J. Biomechanics* **13**, 49–57 (1980).
2. R. Selles, J. B. J. Bussmann, R. C. Wagenaar and H. J. Stan, "Comparing predictive validity of four ballistic swing phase models of human walking", *Journal of Biomechanics* **34**, 1171–1177 (2001).
3. T. McGeer, "Passive dynamic walking", *Int. J. Robot. Res.* **9**, 62–82 (April, 1990).
4. S. H. Collins, M. Wisse and A. Ruina, "A two legged kneed passive dynamic walking robot", *Int. J. Robotics Research* **20**, 607–615 (July, 2001).
5. T. McGeer, "Passive dynamic biped catalogue", *Proc., Experimental Robotics II: The 2nd International Symposium* (R. Chatila and G. Hirzinger, eds.), Berlin (Springer-Verlag, 1992), pp. 465–480.
6. R. Q. van der Linde, "Bipedal walking with active springs, gait synthesis and prototype design", *PhD thesis* (Delft University of Technology, Delft, The Netherlands, November 2001. ISBN 90-370-0193-9).
7. C.-M. Chew and G. A. Pratt, "Dynamic bipedal walking assisted by learning", *Robotica* **20**, Part 5, 477–491 (2002).
8. T. Saidouni and G. Bessonnet, "Generating globally optimised sagittal gait cycles of a biped robot", *Robotica* **21**, No. 2, 199–210 (2003).
9. X. Mu and Q. Wu, "Synthesis of a complete sagittal gait cycle for a five-link biped robot", *Robotica* **21**, No. 5, 581–587 (2003).
10. M. Garica, A. Chatterjee, A. Ruina and M. J. Coleman, "The simplest walking model: Stability, complexity, and scaling", *ASME J. Biomech. Eng.* **120**, 281–288 (April, 1998).
11. A. L. Schwab and M. Wisse, "Basin of attraction of the simplest walking model", *Proc., International Conference on Noise and Vibration*, (Pennsylvania), ASME (2001) Paper number DETC2001/VIB-21363 (9 pages).
12. A. D. Kuo, "Energetics of actively powered locomotion using the simplest walking model", *Journal of Biomechanical Engineering* **124**, 113–120 (February, 2002).
13. M. J. Ijzerman, G. Baardman, H. J. Hermens, P. H. Veltink, H. B. K. Boom and G. Zilvold, "The influence of the reciprocal cable linkage in the advanced reciprocating gait orthosis on paraplegic gait performance", *Prosthetics and Orthotics International* **21**, 52–61 (1997).
14. V. T. Inman, H. J. Ralston and F. Todd, *Human Walking* (Baltimore: Williams & Wilkins, 1981. ISBN 0-683-04348-X).
15. M. Wisse and A. L. Schwab, "A 3d passive dynamic biped with roll and yaw compensation", *Robotica* **19**, 275–284 (2001).

16. M. Wisse and J. van Frankenhuyzen, "Design and construction of mike; a 2d autonomous biped based on passive dynamic walking", *Proc., Conference on Adaptive Motion of Animals and Machines, AMAM*, (Kyoto, Japan) (2003) Paper number WeP-I-1 (8 pages).
17. H. J. Ralston, "Energy-speed relation and optimal speed during level walking," *Int. Z. Angew. Physiol.* **17**, 277–283 (1958).
18. J. P. Meijaard, "Efficient numerical integration of the equations of motion of non-smooth mechanical systems," *Zeitschr. der Angew. Math. Mech.* **77**, 6, 419–427 (1997).
19. C. S. Hsu, *Cell-to-cell Mapping; a Method of Global Analysis for Nonlinear Systems*, Applied mathematical sciences 64 (New York: Springer, 1987. ISBN 0-387-96520-3).

APPENDIX: SIMULATION METHODS AND PROCEDURES

This appendix describes the methods used to simulate the motion of the simplest walker with upper body. In order of appearance after the start of a new walking step, a simulation contains the following aspects: A) equations of motion, B) numerical integration, C) end-of-step (heel strike) detection, and D) heelstrike impact equations. Then the biped starts a new step. For continuous walking, we must study the step-to-step behavior to E) find periodic solutions and F) determine the linearized stability, and finally G) investigate the basin of attraction of these periodic solutions. This section focuses on the current model; the applied simulation method is elaborated in detail in references [11, 15].

A. Equations of motion

The configuration of the walker is defined by the coordinates of the four pointmasses (*stance foot*, *hip*, *swing foot*, and *upper body*), which can be arranged in a global vector $\mathbf{x} = (x_{st}, y_{st}, x_h, y_h, x_{sw}, y_{sw}, x_b, y_b)^T$. In order to obtain a minimal set of equations, the eight coordinates of \mathbf{x} are expressed as functions of the independent coordinates θ and ϕ . To allow inspection of the ground reaction forces, we introduce two more independent coordinates (u and v), representing respectively the x- and y-coordinates (orthogonal to the walking slope) of the stance foot, which will obviously be fixed during the walking motion. The expression of \mathbf{x} as a function of the vector of independent coordinates $\mathbf{q} = (u, v, \theta, \phi)^T$ reads:

$$\mathbf{x} = \mathbf{x}(\mathbf{q}) \rightarrow \begin{bmatrix} x_{st} \\ y_{st} \\ x_h \\ y_h \\ x_{sw} \\ y_{sw} \\ x_b \\ y_b \end{bmatrix} = \begin{bmatrix} u \\ v \\ u - \sin(\theta) \\ v + \cos(\theta) \\ u - \sin(\theta) + \sin(\theta - \phi) \\ v + \cos(\theta) - \cos(\theta - \phi) \\ u - \sin(\theta) - l_b \sin(\theta - \phi/2) \\ v + \cos(\theta) + l_b \cos(\theta - \phi/2) \end{bmatrix}. \quad (2)$$

Notice the use of the term $(\theta - \phi/2)$ from Eq. (1). For the walker the global coordinate related mass matrix is

$$\mathbf{M} = \text{Diag}(m_f, m_f, 1 - m_b, 1 - m_b, m_f, m_f, m_b, m_b), \quad (3)$$

The reduced mass matrix \mathbf{M}_r is created via

$$\mathbf{M}_r = \mathbf{T}^T \mathbf{M} \mathbf{T}, \quad (4)$$

with the Jacobian $\mathbf{T} = \frac{\partial \mathbf{x}}{\partial \mathbf{q}}$ from Eq. (2), which can be automatically generated with a symbolic math package.

The gravity forces, contact forces and the spring torque are combined into a reduced force vector \mathbf{f}_r via

$$\mathbf{f}_r = \mathbf{T}^T [\mathbf{f}_g - \mathbf{M} \mathbf{T}_2] + \mathbf{Q}, \quad (5)$$

with the convective accelerations $\mathbf{T}_2 = \frac{\partial(\mathbf{T}\dot{\mathbf{q}})}{\partial \mathbf{q}} \cdot \dot{\mathbf{q}}$, again obtained automatically. The vector of gravity forces reads

$$\mathbf{f}_g = \mathbf{M} \begin{bmatrix} \sin(\gamma) \\ -\cos(\gamma) \\ \sin(\gamma) \\ -\cos(\gamma) \\ \sin(\gamma) \\ -\cos(\gamma) \\ \sin(\gamma) \\ -\cos(\gamma) \end{bmatrix}, \quad (6)$$

and the spring torque and unknown contact forces are represented in the vector with generalized forces \mathbf{Q} :

$$\mathbf{Q} = \begin{bmatrix} Q_u \\ Q_v \\ 0 \\ -k\phi \end{bmatrix}. \quad (7)$$

This amounts to the reduced equations of motion:

$$\mathbf{M}_r \ddot{\mathbf{q}} = \mathbf{f}_r. \quad (8)$$

The contact condition on the stance foot gives the boundary conditions $u = \text{constant}$ and $v = 0$. This contact is only valid for compressive vertical contact force, $Q_v > 0$, and will be checked during the simulation. The resulting set of linear equations can be solved for Q_u , Q_v , $\ddot{\theta}$ and $\ddot{\phi}$ by numerical evaluation and subsequent solution.

B. Numerical integration

The second order differential equations of motion are numerically integrated using the Runge-Kutta method. It must be taken into account that only two of the generalized coordinates are independent (θ and ϕ), the other two are fixed by the boundary condition of keeping the stance foot at the floor, and should therefore not be incorporated in the numerical integration.

Away from round-off errors, the integration accuracy is estimated according to:

$$q^* - q_{\Delta t} \approx \frac{1}{2^n - 1} (q_{\Delta t} - q_{2\Delta t}), \quad (9)$$

where q^* is the real state after one walking step, $q_{\Delta t}$ is the numerically calculated state, $q_{2\Delta t}$ is the same calculation with twice the integration step size, and $n = 4$ is the order of the integration scheme. Simulation results show that for an integration step size of $\Delta t = 0.05$ the absolute error in the state variables $\{\theta, \phi, \dot{\theta}, \dot{\phi}\}$ after one walking step is smaller than $1 \cdot 10^{-7}$.

C. End-of-step detection

The end of a walking step is defined as the instant that the swing foot makes contact with the floor. This is detected during the simulation by monitoring the swing foot clearance (g)

$$g = v + \cos(\theta) - \cos(\theta - \phi), \quad (10)$$

which is the sixth element of \mathbf{x} in Eq. 2.

However, our model has two straight legs of equal length, and no leg retraction mechanisms. In fact, the model is too simple for the real world. When the swing leg passes the stance leg, the swing foot would inevitably ‘scuff’ the floor. We have to ignore this instance of foot contact, and continue simulation as if the floor were not there, until the ‘real’ heel strike occurs. This is detected if all of the following statements are true:

- g has crossed zero,
- \dot{g} is negative,
- the stance leg has passed the vertical position, and
- the absolute angles of the swing and stance leg have opposite signs.

Now that we know that heel strike must have occurred between the last and the previous integration step (between t_n and t_{n-1}), we must pinpoint the exact instant of contact. This is solved by fitting a third order polynomial through the foot clearance function g , for which we need its derivative which can be automatically generated from the state variables. The polynomial is zero at the time of contact t_c , which we express as the fraction

$$\xi = \frac{t_c - t_{n-1}}{t_n - t_{n-1}}. \quad (11)$$

A fast and accurate approach to calculate $\mathbf{q}(t_c)$, as proposed by Meijaard,¹⁸ is interpolating \mathbf{q} between t_{n-1} and t_n with a third-order interpolation polynomial, since we know both \mathbf{q} and $\dot{\mathbf{q}}$ at these instants:

$$\mathbf{q}(t_c) = \begin{bmatrix} (1 - 3\xi^2 + 2\xi^3) \\ (\xi - 2\xi^2 + \xi^3)\delta t \\ (3\xi^2 - 2\xi^3) \\ (-\xi^2 + \xi^3)\delta t \end{bmatrix}^T \begin{bmatrix} \mathbf{q}(t_{n-1}) \\ \dot{\mathbf{q}}(t_{n-1}) \\ \mathbf{q}(t_n) \\ \dot{\mathbf{q}}(t_n) \end{bmatrix}. \quad (12)$$

The results of this method have the same accuracy as the numerical integration procedure in Section B. The interpolation method is efficient because we avoid solving the equations of motion all together.

D. Impact equations

We assume that the heel strike behaves as a fully inelastic impact (no slip, no bounce). Also, double stance is assumed to occur instantaneously, which is in accordance with observations on existing passive dynamic walking prototypes. As soon as the swing foot hits the floor the stance foot lifts up, not interacting with the ground during impact. The resulting vertical velocity of the lifting foot should then be pointed upwards, which is checked during the simulation. If it points downwards, the assumption was an incorrect and there actually was an interaction between the former stance foot and the floor. Without calculation one can see that in that case the walker comes to a complete stop.

The instantaneous velocity changes during impact can be calculated using the original reduced Equations of motion (8). As described in, reference [11] the impact equations read

$$\begin{bmatrix} \mathbf{M}_r & \mathbf{D}^T \\ \mathbf{D} & \mathbf{0} \end{bmatrix} \begin{bmatrix} \dot{\mathbf{q}}^+ \\ \boldsymbol{\rho} \end{bmatrix} = \begin{bmatrix} \mathbf{M}_r \dot{\mathbf{q}}^- \\ -e \mathbf{D} \dot{\mathbf{q}}^- \end{bmatrix}, \quad (13)$$

with Newtons coefficient of restitution $e = 0$ and the swing foot contact impulses $\boldsymbol{\rho}$. \mathbf{D} represents the partial derivatives of the impact constraints with respect to \mathbf{q} . Since there is no interaction between the old stance foot and the floor during impact, the easiest way to derive the impact equations is by first swapping stance and swing leg coordinates. This must be done anyway before simulating the next step, and by doing this swap immediately before heel strike, the impact constraints become simply $u = \text{constant}$ and $v = 0$, resulting in

$$\mathbf{D} = \begin{bmatrix} 1 & 0 & 0 & 0 \\ 0 & 1 & 0 & 0 \end{bmatrix}. \quad (14)$$

The impact affects only $\dot{\mathbf{q}}$ and leaves \mathbf{q} constant. With the new velocities and the swapped stance and swing leg, the walker is ready for the next walking step.

E. Limit cycle analysis

With the above procedure (numerically integrating equations of motion, impact-detection and calculation and stance-swing leg swapping) the initial conditions $\mathbf{v} = (\dot{\mathbf{q}}, \mathbf{q})$ can be mapped from one step onto the next by a step-to-step function \mathbf{S}^5 :

$$\mathbf{v}_{n+1} = \mathbf{S}(\mathbf{v}_n). \quad (15)$$

A walking cycle is specified by the requirement that the vector of initial conditions \mathbf{v}_n results in identical initial conditions for the subsequent step:

$$\mathbf{v}_{n+1} = \mathbf{v}_n. \quad (16)$$

A vector with initial conditions satisfying this requirement is a cyclic solution \mathbf{v}_c , which maps onto itself:

$$\mathbf{S}(\mathbf{v}_c) = \mathbf{v}_c. \quad (17)$$

A cyclic solution can be found by a linearization of the step-to-step function

$$\mathbf{S}(\mathbf{v} + \Delta \mathbf{v}) \approx \mathbf{S}(\mathbf{v}) + \mathbf{J} \Delta \mathbf{v}, \quad \text{with } \mathbf{J} = \partial \mathbf{S} / \partial \mathbf{v}, \quad (18)$$

and applying a Newton-Raphson iteration procedure, starting with a set of initial conditions \mathbf{v} close to the cyclic solution \mathbf{v}_c

$$\begin{aligned} &\text{repeat} \\ &\quad \Delta \mathbf{v} = [\mathbf{I} - \mathbf{J}]^{-1}(\mathbf{S}(\mathbf{v}) - \mathbf{v}) \\ &\quad \mathbf{v} = \mathbf{v} + \Delta \mathbf{v} \\ &\text{until } |\Delta \mathbf{v}| < \epsilon, \end{aligned} \quad (19)$$

where \mathbf{I} is the identity matrix. The Jacobian \mathbf{J} is calculated by a perturbation method, which involves simulation of a full walking step for every initial condition. The result of this depends on the model parameters and the initial estimate for the solution. If the parameters are such that no cyclic gait exists or if the initial estimate is poor, then the solution will diverge. If the solution converges we find one of possibly multiple cyclic solutions.

F. Local stability

If the walker starts a step exactly with \mathbf{v}_c , it will walk forever. However, if small errors ϵ_n appear, the periodic solution needs to be stable for the robot to maintain gait. The stability is described with the Jacobian \mathbf{J} from the previous subsection, which is the linearized multiplication factor for errors from one step to the next:

$$\mathbf{v}_c + \epsilon_{n+1} = \mathbf{S}(\mathbf{v}_c + \epsilon_n) \approx \mathbf{S}(\mathbf{v}_c) + \mathbf{J}\epsilon_n. \quad (20)$$

Errors will asymptotically die out if all eigenvalues of the Jacobian \mathbf{J} have an absolute value smaller than 1, and in that case the periodic solution is stable for small disturbances.

G. Global stability

The global behavior of the step-to-step function \mathbf{S} can be studied with the aid of the cell mapping method.¹⁹ The region of feasible initial conditions is subdivided into a large number (N) of small cells. All unfeasible initial conditions are regarded as a small number (z) of very large cells, so called *sink cells*. The cells are numbered 1 to $N+z$. By application of the step-to-step function \mathbf{S} to the center of each cell, all of the $N+z$ cells point to initial conditions inside one of the other cells, except the sink cells which point to themselves by definition. Starting with cell 1, a sequence of cells appears by following the pointers. This sequence either ends in a sink cell or in a repetitive cycle. This cycle can consist of one self-repeating cell (a fixed point), or a number of cells (representing an asymmetric gait, Section IV C). The repetitive cycle is identified and all cells in the sequence are labeled as basin of attraction of that cycle. Then the procedure is repeated with all N cells. As soon as a known cell (from a previous sequence) is encountered, the procedure can be stopped, and all cells in that sequence are labeled as basin of attraction of that last cell.

The application of the cell mapping method results in a list with all attractors (cyclic solutions) and classification of all discretization points into this list. Not only period-one walking gaits can be found, also period- k walking gaits. Results of the cell mapping method are as accurate as the discretization; within these tolerances fixed points may come and go. For example, what appears to be a fixed cell might, in fact, be slowly changing initial conditions (smaller changes than the discretization) of subsequent steps.